11. E. A. Auerswald, G. Ludwig, H. Schaller, *Cold Spring Harbor Symp. Quant. Biol.* **65**, 107 (1980).
12. F. Zavala, R. W. Gwadz, F. J. Collins, R. S. Nussenzweig, V. Nussenzweig, *Nature (London)* **299**, 737 (1982).
13. Restriction mapping for this physical map was performed on 0.75 percent agarose horizontal slab gels. The DNA bands were visualized under shortwave ultraviolet light after being stained with ethidium bromide; photographs were made with Polaroid Type 55 positive-negative film. The 4 by 5 inch negatives were enlarged to 10 by 12 inch prints to measure the distance the bands migrated from the origin. At least ten restriction fragments from a phage λ digest with Hind III and Kpn I plus a phage M13mp8 digest with Hae III were used as size marker DNA. A least-squares-fit standard curve was generated with the aid of a computer for the marker DNA's. The individual Tn5 insertions were mapped with respect to the standard curve determined for each gel to generate the physical map.
14. F. Zarala, A. H. Cochrane, E. Nardin, R. S. Nussenzweig, V. Nussenzweig, *J. Exp. Med.*, in press.
15. We thank A. Cochrane for supplying the monoclonal antibodies 2G3 and 5H8, F. Zavala for instruction in the methodology of the IRMA, and R. Nussenzweig, V. Nussenzweig, and F. Zavala for critically reviewing the manuscript. Supported by UNDP–World Bank–World Health Organization Special Programme for Research and Training in Tropical Diseases [T16/181/M2/27(61)] to G.N.G. and New York University Institutional Funds to G.N.G. L.S.O. is a recipient of a fellowship from the Brazilian National Research Council. J.E. is the recipient of an NIH training grant. J.R.L. is a recipient of an NIH medical scientist in-training grant.

15 February 1983

Intermolecular Interactions in Collagen Self-Assembly as Revealed by Fourier Transform Infrared Spectroscopy

Abstract. *When a solution of collagen molecules, at neutral* p*H and moderate ionic strength, is warmed from 4° to 30°C, a spontaneous self-assembly process takes place in which native-type collagen fibers are produced. Events occurring during thermally induced fibrillogenesis process can be monitored, in aqueous media and in real time, by Fourier transform infrared spectroscopic techniques. Tentative assignments of observed spectral bands are given.*

Although there have been many studies of the fibrillogenesis reaction in vitro (*1, 2*), neither the mechanism of interaction nor the mode of initial assembly has been explained. The groups currently investigating this problem have taken different positions (*3–11*) with regard to the assembly mechanism. This report describes our studies of the collagen self-assembly process with a Fourier transform infrared spectrometer equipped for thermal-jump experiments.

The thermally induced self-assembly reaction involves two clearly distinguishable phases. First, a lag period occurs during which neither the solution turbidity nor the viscosity appears to change (*3, 4*), but during which some alteration in the solution properties must occur. A growth phase follows in which the turbidity increases rapidly and distinct fibrillar structures appear. Analysis of the nature of the interactions in the lag phase has been difficult because the methods used have perturbed the solution, have induced artifacts, or were insufficiently sensitive to detect the onset of interactions.

Helseth and Veis (*6*) suggested that two events might be of particular importance in fibrillogenesis: (i) a temperature-dependent intramolecular conformational change in the structure of the telopeptide regions, and (ii) a change in conformation of weak flexible regions within the triple helix, cooperatively assisted by intermolecular interactions with the telopeptides. Such interactions would be accompanied by changes in hydrogen bonding and bond strength.

Previous investigations of collagen structure by infrared spectroscopy were not directed to study of the mechanism of fibrillogenesis (*12–14*). The use of dry films meant that the studies began after collagen fibrils had already formed, so that no information on the collagen fibril aggregation process could be obtained. Therefore, these studies monitored the collagen-gelatin denaturation instead of the aggregation process. Moreover, the dry film studies could not address an important aspect of the physiological environment—the presence of buffered aqueous solutions. Dry collagen films have been studied in a highly humid or moist atmosphere (*15*). However, these data only demonstrate the absorption of water on collagen and not the effects of water solvation on collagen during fibrillogenesis. Raman studies have been carried out in both H_2O and D_2O solutions (*16*), but no attempt has been made to follow the fibrillogenesis process.

Fourier transform infrared (FTIR) spectroscopy, in which the hydrogen bond–related amide I, II, and III bands can be observed in H_2O, appeared to be an attractive nonperturbing means of studying both the lag and growth phases during self-assembly. The sensitivity of the method, which could be enhanced by accumulating scans over time intervals short compared to the kinetic processes being studied, was also promising. As described below, a system has been devised in which self-assembly can be followed directly in a thermostated infrared transmission cell.

Neutral salt–soluble collagen was extracted from lathyritic rat skin or tendon according to the protocol of Helseth and Veis (*6*). This collagen is essentially monomeric in solution and has a minimal content of β and γ components after denaturation. The gelation system of Comper and Veis (*3*), with 0.0327*M* KH_2PO_4 at *p*H 7.03, was used. In the experiment described below, the rat skin collagen concentration was 2.1 mg/ml and the ionic strength was adjusted to 0.15 with NaCl. This relatively high collagen concentration was used in all studies to maximize the infrared intensities. Under these conditions the turbidimetric lag, as determined with a double-beam spectrophotometer at 430 nm, was 3 to 5 minutes. The temperature jump from 3° to 30°C required 8 to 11 minutes (2 to 3 minutes to go from 3° to 28°C, the remainder to equilibrate to 30°C).

In the FTIR studies described here, similar temperature jump experiments were conducted in a standard transmission infrared cell from Harrick Scientific Corporation (Ossining, New York). The transmission cell temperature was maintained with a copper cooling coil wrapped around the cell housing. A heat transfer paste (Ecotherm TC-4, Emerson and Cummins Inc., Canton, Massachusetts) was applied to the cooling coil, housing, and cell window to promote rapid heating of the cell. The metal cell support plate was replaced by a Teflon support of similar size to decrease conductive heat transfer losses. The thermal gelatin temperature (30°C) was a compromise designed (i) to extend the lag period to several minutes, but (ii) to hold the temperature difference between the cell and the interferometer compartment (35°C) to a minimum.

In this transmission cell a period of 7 to 10 minutes was required to raise the cell temperature from 3° to 30°C (4 to 5 minutes to go from 3° to 28°C, the remainder to equilibrate to 30°C), nearly the same time as required for the temperature jump studies in the ultraviolet spectrophotometer. Temperature measurements were made in the FTIR cell with a thermocouple placed in a well drilled into the window at its periphery. A thermal gradient across the window could lead to a difference of perhaps 1° to 2° between the recorded cell temperature and the actual collagen solution temperature. This recorded cell temperature also takes into account any possible heating effects from the infrared radiation.

The infrared spectra were obtained

with a Digilab FTS-10 Fourier transform infrared system modified for rapid scan (Digilab, Cambridge, Massachusetts). The instrument continuously collected scans during the heating period and for 60 minutes after the temperature reached 30°C. Spectra were collected about every 15 seconds during the early heating period. This should ensure that enough data points were gathered so that changes could be observed during the 3- to 5-minute lag period. Control experiments were conducted in which the cell was filled with phosphate-buffered saline at the same concentration as for the test with collagen. Reference spectra from these control tests, taken at corresponding temperatures and times, were subtracted from the collagen solution spectra. With the instrument and experiment conditions used, frequencies and relative intensity changes were reproducible to about 1 cm^{-1} and 10 percent, respectively. Peak height intensities and half-bandwidths were measured from the amide I and amide II bands, using a baseline from 1490 to 1720 cm^{-1}.

The spectrum of the collagen is shown in Fig. 1A for the initial solution at 3°C and after fibril assembly was completed at the end of the heating period. Spectra are shown only for the range 1800 to 1100 cm^{-1} because the OH stretching vibration of H_2O (near 3300 cm^{-1}) for both the collagen solution and the reference saline is so intense that accurate subtraction is not possible. Therefore, the collagen NH stretching vibrations (near 3300 cm^{-1}) were not observed. The OH bending vibration of H_2O (near 1640 cm^{-1}) was of sufficiently low intensity that accurate subtraction was possible. Thus, the collagen infrared bands below 1800 cm^{-1} could be observed down to 1000 cm^{-1}, where the cutoff points of the infrared cell windows and the mercury-cadmium-telluride detector established a lower limit. Strong amide I (1650 cm^{-1}), amide II (1560 cm^{-1}), and amide III complex (1330 to 1240 cm^{-1}) bands were observed. These bands contain most of the information about protein structure and conformation. Standard frequency assignments for proteins and polypeptides for amide I and amide III bands would be: 1650 cm^{-1} (amide I) and 1242 cm^{-1} (amide III) for native collagen (*17*); 1650 cm^{-1} (I) for denatured collagen (*17*); 1665 cm^{-1} (I) and 1250 cm^{-1} (III) for random coil (*18*); 1650 to 1655 cm^{-1} (I) and 1260 to 1290 cm^{-1} (III) for α helix (*18*); and 1630 cm^{-1} (I) and 1235 cm^{-1} (III) for β sheet. In comparing the spectra at different temperatures, it was evident that band frequencies, half-widths, and intensities were changing.

Table 1. Characteristics of the amide I and amide II bands during collagen fibrillogenesis.

Spectrum	Amide I			Amide II		
	Frequency (cm^{-1})	Intensity (arbitrary units)	Half-bandwidth (cm^{-1})	Frequency (cm^{-1})	Intensity (arbitrary units)	Half-bandwidth (cm^{-1})
No. 1, native collagen monomer	1655	1.6	57	1559	0.57	33
No. 37, midst of lag phase	1651	1.7	60	1559	0.55	31
No. 99, completed fibrils	1651 (1640 sh*)	1.2	61	1555	0.47	32

*Shoulder (sh) on side of 1651 cm^{-1} infrared band.

As indicated above, scans were taken at regular intervals during fibril aggregation. Figure 1, B and C, shows the spectra observed just as the starting material reached the gelation, self-assembly temperature of 30°C (spectrum 37), as well as the initial 3°C data (spectrum 1) and the final state after 60 minutes at 30°C (spectrum 99). We estimate that spectrum 37 represents the state of the collagen toward the end of the lag phase, while spectrum 99 includes changes during the growth period.

Figure 1B shows the region 1800 to 1400 cm^{-1}, including the amide I and amide II bands. The characteristic features of these bands are presented in Table 1. Comparing the numbers in Table 1 for spectra 1 and 37 it is seen that amide II did not change in frequency, intensity, or half-bandwidth during the lag period. However, during the fibril growth stage the amide II frequency shifted downfield and the intensity decreased. In contrast, the amide I band showed distinct changes during both the lag period and the fibril growth stage. The amide I shifted from 1655 to 1651 cm^{-1} and became somewhat broadened during the lag period. As fibrils formed, a shoulder at 1650 cm^{-1} became apparent on the side of the 1651 cm^{-1} amide I band and the maximum intensity decreased.

The amide III region (Fig. 1C) showed the most striking changes. In spectrum 1, the 3°C soluble monomer amide III band at 1257 cm^{-1} was more intense than the 1242 cm^{-1} band. In the lag phase (spectrum 37) the intensity ratio was reversed. After fibril growth the total intensity of all amide III bands showed a major increase (spectrum 99), and the 1242/1257 intensity ratio was so high that the 1257 cm^{-1} band was only a shoulder on the side of the 1242 cm^{-1} band. Smaller changes can be seen in the region 1260 to 1310 cm^{-1} during both the lag and

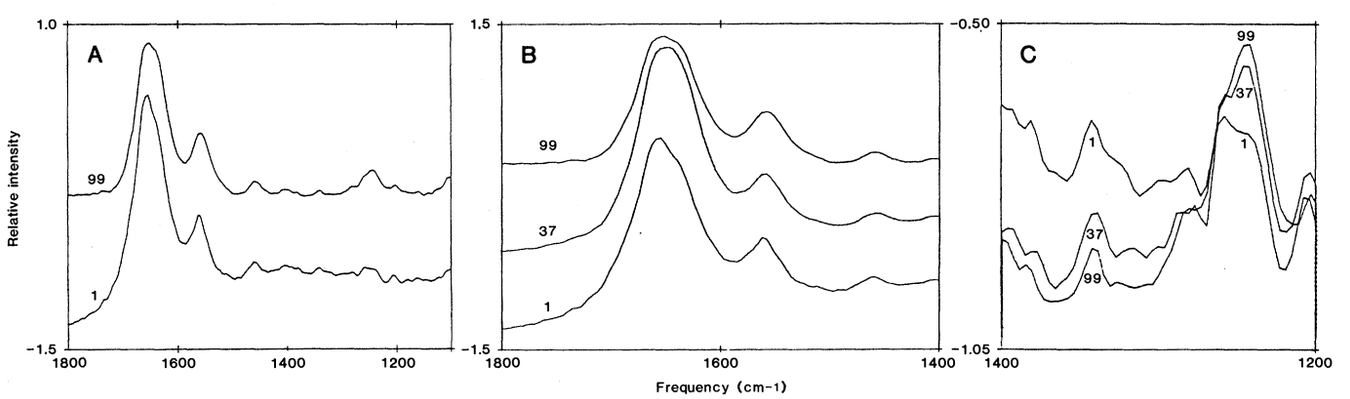

Fig. 1. Infrared spectra: (A) monomeric (No. 1) and thermally aggregated (No. 99) rat skin collagen; (B) collagen at different temperatures (1, 3°C; 37, 30°C; and 99, 30°C after 60 minutes); and (C) collagen showing amide III region at different temperatures (1, 3°C; 37, 30°C; and 99, 30°C after 60 minutes).

growth phases. These bands might be part of the α-helix amide III bands or might arise from vibrations of protein other than those involving the amide groups.

The triple helical region that comprises the bulk of the native collagen molecule has a structure distinctly different from the α-helix or β-sheet structures of other proteins and polypeptides. Thus, the spectral band assignments mentioned previously cannot be used without a great deal of caution.

The point of this report is not to explain the spectral changes observed during collagen fibrillogenesis, but rather to point out the wealth of detail that can be observed by FTIR in this clean system and the ability to dynamically detect subtle changes which reflect both intramolecular configurational and intermolecular packing alterations. It is nevertheless tempting to speculate that the appearance of the 1640 cm^{-1} shoulder on the amide I and the broadening seen in the lag phase are indicative of conformational changes in the telopeptides, while the increase in the amide III band at 1242 cm^{-1} with fibril growth may indicate the perfection of the triple helix. This was suggested by Helseth and Veis (*6*) as the consequence of telopeptide-collagen helix packing. Identification of the structural origins of these spectral changes and the use of this technique to elucidate the mechanisms of fibrillogenesis will require significantly more study, but FTIR techniques are directly applicable to protein interaction studies in aqueous solution.

R. J. JAKOBSEN
L. L. BROWN
Biological Spectroscopy Facility, Battelle, Columbus Laboratories, Columbus, Ohio 43201

T. B. HUTSON
D. J. FINK
Medical and Molecular Biology, Battelle, Columbus Laboratories

A. VEIS
Department of Oral Biology, Dental School, Northwestern University, Chicago, Illinois 60611

References and Notes

1. J. Gross, J. H. Highberger, F. O. Schmitt, *Proc. Natl. Acad. Sci. U.S.A.* **41**, 1 (1955).
2. G. C. Wood, *Int. Rev. Connect. Tissue Res.* **2**, 1 (1965).
3. W. D. Comper and A. Veis, *Biopolymers* **6**, 2113 (1977).
4. ———, *ibid.*, p. 2133.
5. D. L. Helseth, J. A. Lechner, A. Veis, *ibid.* **18**, 3005 (1979).
6. D. L. Helseth and A. Veis, *J. Biol. Chem.* **256**, 7118 (1981).
7. R. A. Gelman, B. R. Williams, K. A. Piez, *ibid.* **254**, 180 (1979).
8. R. A. Gelman, D. C. Poppke, K. A. Piez, *ibid.*, p. 11741.
9. F. H. Silver and R. L. Trelstad, *J. Theor. Biol.* **81**, 515 (1979).
10. F. H. Silver, K. H. Langley, R. L. Trelstad, *Biopolymers* **18**, 2523 (1979).
11. T. Hayashi, *J. Biochem. (Toyko)* **87**, 1037 (1980).
12. I. V. Yannas, *J. Macromol. Sci. Rev. Macromol. Chem.* **7**, 49 (1972).
13. A. Huc and J. Sanijouand, *Biochim. Biophys. Acta* **154**, 408 (1968).
14. P. L. Gordon, C. Huang, R. C. Lord, I. V. Yannis, *Macromolecules* **7**, 954 (1974).
15. H. Susi, J. S. Ard, R. Carroll, *J. Biopolym.* **10**, 1597 (1971).
16. B. G. Frushour and J. L. Koenig, *Biopolymers* **14**, 379 (1975).
17. S. Ghosh and A. Veis, in *Photographic Gelation*, R. J. Cox, Ed. (Academic Press, London, 1972), pp. 3–12.
18. R. C. Lord and T. R. Mendelsohn, in *Membrane Spectroscopy*, E. Grall, Ed. (Springer-Verlag, Berlin, 1981), p. 400.

8 March 1982; revised 29 November 1982

Localization of Wheat Germ Agglutinin–Like Lectins in Various Species of the Gramineae

Abstract. *Antigenically similar chitin-binding lectins are present in the embryos of wheat, barley, and rye, members of the Triticeae tribe of the grass family (Gramineae). However, the lectins display different localization patterns in these embryos. Lectin is absent from the coleoptile of barley but is present in the outer surface cells of this organ in wheat and in both inner and outer surface cells of rye coleoptiles. All three cereals contain lectin at the periphery of embryonic roots. Similar lectins were not detected in oats and pearl millet, members of other tribes of the Gramineae. Rice, a species only distantly related to wheat, contains a lectin that is antigenically similar to the other cereal lectins and located at the periphery of embryonic roots and throughout the coleoptile.*

Barley and rye embryos contain *N*-acetylglucosamine (GlcNAc)-binding lectins that are virtually indistinguishable by biochemical and immunological criteria from the well-characterized wheat lectin, wheat germ agglutinin (*1*). Although their function is not known, evolutionary conservatism such as this suggests that these lectins perform adaptationally significant roles in the plants in which they are found. We reported earlier that the wheat lectin is localized in peripheral portions of wheat embryos, that is, in the root cap, coleorhiza, and the outer layers of the radicle, coleoptile, and scutellum (*2*). We have sought to determine whether the barley and rye lectins are similarly localized.

Antiserum to wheat germ agglutinin (WGA) was prepared as described (*3*). In order to determine whether this antiserum was able to cross-react with lectins from other grasses, we prepared extracts of wheat, barley, and rye embryos as described (legend to Fig. 1). Results obtained with our antiserum to WGA were similar to those reported by Peumans *et al.* (*1*). After Ouchterlony double diffusion of these extracts against antiserum to WGA, precipitin arcs of identity formed between the wheat, rye, and barley extracts (Fig. 1).

We identified WGA-like lectins in sections of these grass species with the peroxidase-antiperoxidase procedure (Fig. 2)

Fig. 1. Diffusion of grain extracts against antiserum to WGA. Wheat, barley, rye, and oat grains were soaked in distilled water overnight at 4°C. Fifty embryos of each species were excised, ground in a mortar with 6 ml of 50 m*M* HCl, and shaken for 4 hours at 4°C. The mixtures were centrifuged at 10,000*g* for 15 minutes, after which the supernatants were collected and brought to 50 percent saturation with ammonium sulfate. After standing overnight at 4°C, the precipitates were pelleted by centrifugation, suspended in 1 ml of distilled water, and dialyzed against distilled water. A hemagglutination assay, performed as described (*3*), revealed titers of 64, 64, and 32 for the wheat, barley, and rye extracts, respectively. These activities were totally inhibited by oligomers of GlcNAc. The oat embryo extracts displayed no hemagglutinating activity. Double diffusion was performed in 1 percent agarose gels prepared in 50 m*M* barbital buffer (*p*H 8.6), with 100 m*M* GlcNAc included to inhibit precipitation caused by lectin-sugar interactions. The gels were dried and stained with Coomassie blue before being photographed. Monospecific immunoglobulins to WGA (10 μl of a solution containing 1 mg/ml) were loaded into the center well and (counterclockwise beginning at well 1) purified WGA, or extracts of wheat, barley, rye, and oat embryos were added to the peripheral wells. Note the fusion of the precipitin arcs of the wheat, barley, and rye extracts, and the absence of a precipitation reaction between antiserum to WGA and the oat extract.